

M.V. Popovych, A.V. Stronski, K.V. Shportko

## Structural properties of Ga<sub>11.7</sub>Ge<sub>14.1</sub>Te<sub>74.2</sub> alloys

*V.Lashkaryov Institute of Semiconductor Physics NAS Ukraine, Kyiv, Ukraine, [Niva94@ukr.net](mailto:Niva94@ukr.net)*

In the present paper the amorphous Ga<sub>11.7</sub>Ge<sub>14.1</sub>Te<sub>74.2</sub> alloys have been studied by X-ray diffraction and Raman spectroscopy. The experimental X-ray diffraction patterns were used for calculations of radial distribution functions which have given the positions of the nearest-neighbour bond length  $r_1$ - 2.67 Å and second-neighbour bond length  $r_2$  - 4.27 Å. Similar  $r_1$  values were observed for Ga-Ge-Te glasses of other compositions. Observed bands in the Raman spectra of Ga<sub>11.7</sub>Ge<sub>14.1</sub>Te<sub>74.2</sub> samples show that such glass contains different nanophases and can be explained in the terms of vibrational modes of Ga-Te and Ge-Te glasses and films. Investigations of compositional dependencies of characteristic constituent Raman bands intensities whose concentration is changing with the composition are necessary in order to obtain better assignment of Raman bands.

**Keywords:** chalcogenide glasses, X-ray diffraction, radial distribution function, Raman spectroscopy, nanophases.

*Received 07 July 2022; Accepted 05 December 2022.*

### Introduction

Chalcogenide thin films and composites on their base are used as the recording medium for fabrication of optical elements, in holography and phase change-type optical memory discs, integrated and fiber optics, sensors, etc. [1-19] This is due to their possession of unique characteristics such as wide range of optical transparency, high refractive index and photo structural transformations, accompanied by the change of optical and chemical properties [2-5]. Among the number of different photo-induced effects are photo-darkening and bleaching, local expansion or contraction, changes of the refractive index, polarization-dependent structural changes, photoinduced dichroism [1-2, 4-5]. In recent times, studies of nanocomposite materials based on chalcogenide glasses have been actively conducted [6, 11, 13-14]. Such nanocomposite materials provide possibility of the direct recording of surface reliefs (without step of selective etching), recording process depends on the polarization of the recording beams.

Family of GaGeTe alloys is interesting due to versatile far-IR optics [7-10], phase change-type optical memory [15-16] and sensor [17] applications. The structural features of chalcogenide glasses and films are

important for various characteristics and processes, including photoinduced ones. The addition of Ga to GeTe alloys can influence crystallization timings and room-temperature stability [20]. Accordingly, better understanding of the structural properties can help in the optimization of the sensitivity and relief formation processes of composite nanomultilayer structures based on chalcogenide glasses, which are promising for the direct recording of optical elements.

The better understanding of the correlations between their structural and macroscopic properties and the information on the short-range order structure of chalcogenide glasses is needed. This was the main motivation to study Ga<sub>11.7</sub>Ge<sub>14.1</sub>Te<sub>74.2</sub> alloys.

### I. Experimental

Studied bulk Ga<sub>11.7</sub>Ge<sub>14.1</sub>Te<sub>74.2</sub> alloys were prepared by the conventional melt quenching technique. Proper quantities of high-purity (99.999%) elements, vacuum sealed into a quartz ampoule, were kept in a furnace at ~ 1000 °C for about 30 h, shaken for homogeneous mixing and then quenched in cold water.

X-ray diffraction patterns samples were recorded with

use of the X-ray diffractometer with Bragg–Brentano geometry, using Cu  $K_\alpha$  radiation 1.54178 Å and mounted graphite monochromator for a diffracted beam. The diffraction data were collected in the range of scattering vector magnitudes  $Q$  between 0.4 and 8 Å<sup>-1</sup>.  $Q = \frac{4\pi \sin \theta}{\lambda}$ .

All samples were examined in transmission geometry. All the X-ray experiments were performed at ambient temperature. The diffraction intensities were corrected for the background, incoherent (polarization and absorption) and multiple scattering in the usual ways in order to eliminate the part of radiation which does not carry structural information. The spectra were measured at a constant rate. The Compton scattering was corrected using the values given by Balyuzi and Faber-Ziman [21-22], total structure factor  $S(Q)$  was calculated from the scattering intensity as

$$S(Q) = \frac{I_{\text{coh}} - \{ \langle f^2(Q) \rangle - \langle f(Q) \rangle^2 \}}{\langle f(Q) \rangle^2}$$

with  $\langle f^2(Q) \rangle = \sum_i c_i f_i^2(Q)$ ,  $\langle f(Q) \rangle = \sum_i c_i f_i(Q)$  where  $c_i$  is the molar fraction and  $f_i$  is the total atomic scattering factor of the  $i$ -th component of the glass.

After Fourier transformation the reduced radial distribution functions  $G(r)$  (RDF) were determined, the measured  $S(Q)$  using the fast Fourier transform technique [23-26] as follows:

$$G(r) = \frac{2}{\pi} \int_0^\infty (S(Q) - 1) Q \sin(Qr) dQ \quad (1)$$

In reality, the data should be multiplied by a modification factor in order to reduce the ripples inevitably introduced due to the finite accessible upper  $K$  value ( $K_{\text{max}}$ ) in the measurements. Eq.(1) therefore becomes

$$G(r) = \frac{2}{\pi} \int_0^{Q_{\text{max}}} (S(Q) - 1) Q M(Q) \sin(Qr) dQ \quad (2)$$

where  $M(K)$  is called the damping factor [25-26] and is given by

$$M(Q) = \frac{\sin\left(\frac{\pi Q}{Q_{\text{max}}}\right)}{\frac{\pi Q}{Q_{\text{max}}}} \quad Q \leq Q_{\text{max}}, \\ = 0, \quad Q > Q_{\text{max}}$$

$G(r)$  may also be expressed directly in real space coordinates to emphasize its relationship with the local atomic density,  $\rho(r)$  at a distance  $r$  and the bulk atomic density,  $\rho_0$ ; as follows

$$G(r) = 4\pi r (\rho(r) - \rho_0) \quad (3)$$

where  $\rho(r)$  is the density function, which represents an atomic pair correlation function, and is equal to zero at values of  $r$  less than the average nearest neighbor interatomic separation and equal to the average value of density  $\rho_0$  at very large value of  $r$ , where the material becomes homogenous. In between these two limits,  $\rho_0$  for an amorphous solid will exhibit an oscillatory behavior, with peaks in the probability function representing the

average interatomic separations. At short distances ( $r \leq 2\text{Å}$ ), see Eq.(3),  $G(r)$  should follow the density line ( $-4\pi r \rho_0$ ) which is used as a quality check of the data [25-26].

The radial distribution function,  $RDF(r)$ , is defined as the number of atoms lying at distances between  $r, r + dr$  from center of an arbitrary origin atom and written as

$$RDF(r) = rG(r) + 4\pi r^2 \rho_0 = 4\pi r^2 \rho(r) \quad (4)$$

The function that is used in the determination of atomic distances and co-ordination numbers is the total distribution function,  $T(r) = \frac{RDF(r)}{r} = 4\pi r \rho(r)$ . The average coordination number,  $N$ , in a spherical shell between radius  $r_1$  and  $r_2$  around any given atom, can be calculated as the number of atoms in the area between  $r_0$  and  $r'$ , where  $r_0$  is a lower limit of  $r$ , below which  $\rho(r)$  is zero, and  $r_0$  is the first minimum of  $4\pi r^2 \rho(r)$ . The position of the first peak gives a value for the nearest-neighbour bond length,  $r_1$ , and similarly, the position of the second peak gives the next neighbour distance,  $r_2$ . The RDF yields only a limited amount of information, restricted essentially to the local structure around a given atom, i.e. bond lengths and bond angles. A knowledge of both bond length  $r_1$  and  $r_2$  yield the value of the bond angle  $\theta$ , given by [27]:

$$\theta = 2 * \sin^{-1}\left(\frac{r_2}{2*r_1}\right) \quad (5)$$

Raman spectra of Ga<sub>11.7</sub>Ge<sub>14.1</sub>Te<sub>74.2</sub> samples were measured in the spectral range from 50 to 400 cm<sup>-1</sup> at room temperature using a FRA-106 Raman attachment to Bruker IFS 88 applying the diode pump Nd:YAG laser of ca. 100 mW power and using the liquid nitrogen-cooled Ge detector with the resolution set to 1 cm<sup>-1</sup> with 256 scans collected in each experiment.

## II. Results and Discussion.

### Radial Distribution Functions

The X-ray diffractograms of Ga<sub>11.7</sub>Ge<sub>14.1</sub>Te<sub>74.2</sub> alloys were used for calculation of radial distribution functions (RDF). RDF for studied alloys were obtained using program the RAD GTK+ [28] and are presented in Fig.1. The positions of the nearest-neighbour bond length  $r_1$  was 2.67 Å and  $r_2$  - 4.27 Å. Similar  $r_1$  values were observed for Ga-Ge-Te glasses of other compositions. The values of the  $r_2/r_1$  ratio are close to 1.63 which is a typical value for a regular tetrahedron structure. EXAFS studies of a-GeTe [29] have shown that the Ge–Te distance is about 2.65 Å. For GaGeTe systems according to [30] Te-Ga bonds lengths were estimated as 2.67 Å. Similar values for Ga-Te bonds in GaTe (2.64–2.69 Å) were obtained in [31] and 2.67 Å for Ga<sub>25</sub>Te<sub>75</sub> in [15].

The bond angle values  $\theta = 106^\circ$  calculated using eq. (5) for Ga<sub>11.7</sub>Ge<sub>14.1</sub>Te<sub>74.2</sub> alloys is in good agreement with other published data on GaGeTe alloys [32].

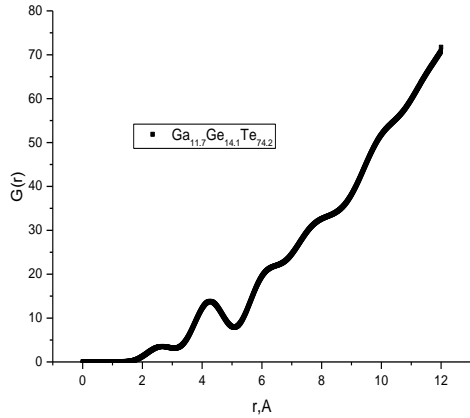


**Fig. 1.** Radial distribution functions of  $\text{Ga}_{11.7}\text{Ge}_{14.1}\text{Te}_{74.2}$  glasses.

### Raman spectra.

The Raman spectra of  $\text{Ga}_{11.7}\text{Ge}_{14.1}\text{Te}_{74.2}$  samples and decomposition on the constituent bands presented in Fig. 2 exhibit main bands:  $88\text{ cm}^{-1}$ ,  $104\text{ cm}^{-1}$ ,  $115\text{ cm}^{-1}$ ,  $125\text{ cm}^{-1}$ ,  $136\text{ cm}^{-1}$  and a band structure around  $160\text{ cm}^{-1}$ . Observed bands in the Raman spectra of  $\text{Ga}_{11.7}\text{Ge}_{14.1}\text{Te}_{74.2}$  samples can be explained in the terms of vibrational modes of Ga-Te and Ge-Te glasses [33-47]. The band at  $88\text{ cm}^{-1}$  in spectrum, is ascribed to GeTe vibration modes (bending modes of  $\text{GeTe}_4$  ( $\text{GaTe}_4$ ) tetrahedral) [34-39] or trigonal Te [40]. The band at  $104\text{ cm}^{-1}$  is characteristic to the trigonal Te [40]. Raman spectra for the annealed  $\text{GeTe}_2$  films have two broad Raman bands from  $110\text{--}135\text{ cm}^{-1}$  and  $135\text{--}145\text{ cm}^{-1}$  with a maximum at  $121\text{ cm}^{-1}$  and  $141\text{ cm}^{-1}$  and an additional Raman band is noticed at  $156\text{ cm}^{-1}$  [33]. The Raman band obtained at  $121\text{ cm}^{-1}$  is assigned to A1 mode of  $\text{GeTe}_4$  tetrahedral unit [41]. Raman data for bulk Ga-Te glasses [15] assign  $109\text{ cm}^{-1}$  band to symmetric Ga-Te breathing mode,  $124\text{--}135\text{ cm}^{-1}$  range - corner-sharing (CS) or edge-sharing (ES)  $\text{GaTe}_4$  tetrahedra breathing modes,  $156\text{ cm}^{-1}$  mode to Te-Te

stretching modes. Raman spectra of the as-deposited and annealed Ge-Ga-Te films covering the region  $100\text{--}200\text{ cm}^{-1}$  consist of the following features: two main bands located at  $120\text{ to }125\text{ cm}^{-1}$  (peak A) and  $150\text{ to }155\text{ cm}^{-1}$  (peak B) and for annealed films peak C ( $141\text{ cm}^{-1}$ ) [42]. Peak A can be assigned to stretching mode of  $[\text{GeTe}_4]$ , eventually  $[\text{GaTe}_4]$  tetrahedral [42-43] or Te-Te vibrations bonds [36, 42, 44], peak C at  $141\text{ cm}^{-1}$  can be assigned to crystalline Te phase [42, 44-46].

In Raman spectra of GeTe films deposited at different temperatures [34] peaks at  $88$ ,  $120$ ,  $139$ , and  $160\text{ cm}^{-1}$  are found. The broad peaks found at  $88$  and  $160\text{ cm}^{-1}$  are contributed by GeTe vibration modes [35-37]. Two distinct peaks were also observed at  $120$  and  $139\text{ cm}^{-1}$ . It is known that crystalline Tellurium has strongest peaks at  $120.4\pm 0.5$  and  $140.7\pm 0.5\text{ cm}^{-1}$  [47]. The close proximity of the observed peaks suggests the presence of homopolar Te-Te bonds in the as-deposited GeTe films. In the Raman spectra of a-GeTe four main bands appear in the frequency range  $50\text{--}250\text{ cm}^{-1}$  (with approximate wavenumber positions of these bands are as follows: band A,  $\sim 83\text{ cm}^{-1}$ ; band B,  $\sim 125\text{ cm}^{-1}$ ; band C,  $\sim 162\text{ cm}^{-1}$ ; band D,  $\sim 218\text{ cm}^{-1}$ ) [35]. It was noted, that bands A, B and C are certainly combinations of at least two individual peaks each.

The frequency assignments of known structural units in glasses were used to perform the peak-fitting analyses and to compare the relative contribution of each structural unit in the spectrum of amorphous  $\text{Ga}_{11.7}\text{Ge}_{14.1}\text{Te}_{74.2}$  alloys. It is necessary to note that a larger number of vibrational modes contribute to the overall spectrum. We allowed upon fitting the Raman spectra a maximum  $2\text{--}3\text{ cm}^{-1}$  displacement of the peak from the position of the peaks known from the reference literature. Tentative Gaussian decomposition of Raman spectra of  $\text{Ga}_{11.7}\text{Ge}_{14.1}\text{Te}_{74.2}$  alloy is shown in Fig. 2. Assignments of particular bands detected in Raman spectra of  $\text{Ga}_{11.7}\text{Ge}_{14.1}\text{Te}_{74.2}$  samples are summarized in Table 1.

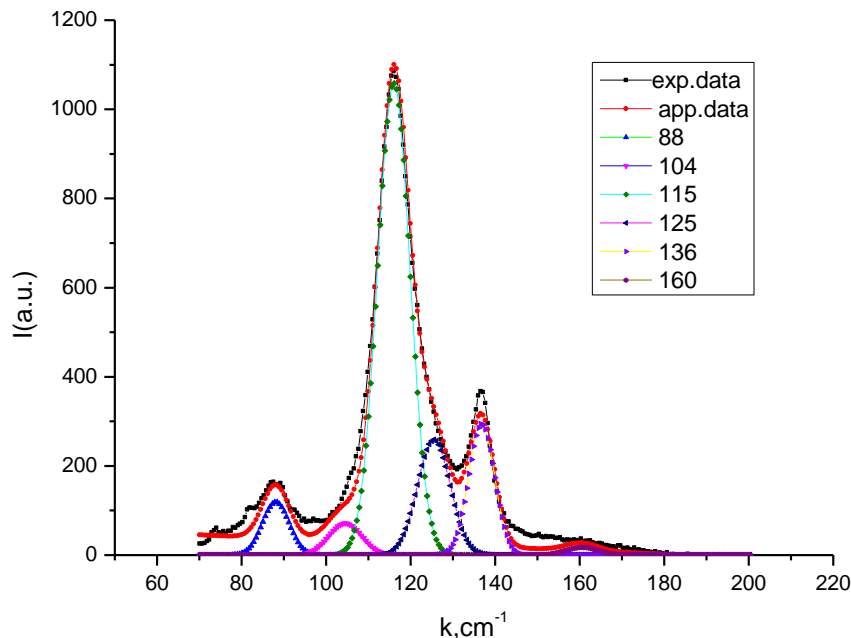


**Fig. 2.** Raman spectra of studied  $\text{Ga}_{11.7}\text{Ge}_{14.1}\text{Te}_{74.2}$  chalcogenide glasses.

**Table 1**

Assignment of particular bands detected in Raman spectra of Ga-Ge-Te, Ge-Te, Ga-Te, Te samples.

Wave number, cm <sup>-1</sup>	Assignment	References
88 cm <sup>-1</sup>	GeTe vibration modes Trigonal Te	[34-38] [40]
92 cm <sup>-1</sup>	bending modes of GeTe <sub>4</sub> (GaTe <sub>4</sub> ) tetrahedral	[38-39]
104 cm <sup>-1</sup>	Te modes	[40]
109 cm <sup>-1</sup>	symmetric Ga-Te breathing mode	[15]
115-125 cm <sup>-1</sup>	(peak A) stretching mode of [GeTe <sub>4</sub> ], [GaTe <sub>4</sub> ] tetrahedral units	[42, 43]
120.4±0.5 cm <sup>-1</sup>	Te-Te bonds	[47]
121 cm <sup>-1</sup>	A1 mode of GeTe <sub>4</sub> tetrahedral unit	[41]
124-135 cm <sup>-1</sup>	corner-sharing (CS) or edge-sharing (ES) GaTe <sub>4</sub> tetrahedra breathing modes	[15]
141 cm <sup>-1</sup>	(peak C) crystalline Te phase	[42, 44-46]
140.7±0.5 cm <sup>-1</sup>	Te-Te bonds	[47]
150-155 cm <sup>-1</sup>	(peak B) Te-Te vibrations bonds	[36, 44]
156 cm <sup>-1</sup>	(peak B) Te-Te stretching modes	[15]
160 cm <sup>-1</sup>	(peak B) GeTe vibration modes	[34-37]

## Conclusions

In the present paper the amorphous Ga<sub>11.7</sub>Ge<sub>14.1</sub>Te<sub>74.2</sub> alloys have been studied by X-ray diffraction and Raman spectroscopy. The experimental X-ray diffraction patterns were used for calculations of radial distribution functions which have given the positions of the nearest-neighbour bond length  $r_1 = 2.67$  Å and  $r_2 = 4.27$  Å. Obtained  $r_1$  values are in good agreement with known from reference literature Ge-Te and Ga-Te bonds lengths, similar  $r_1$  values were observed for Ga-Ge-Te glasses of other compositions. Observed bands in the Raman spectra of Ga<sub>11.7</sub>Ge<sub>14.1</sub>Te<sub>74.2</sub> samples show that such glass contain different nanophases and can be explained in the terms of

vibrational modes of Ga-Te and Ge-Te glasses and films. Investigations of compositional dependencies of characteristic constituent Raman bands intensities whose concentration is changing with the composition are necessary in order to obtain better assignment of Raman bands.

**Popovych M.V.** – junior researcher of the department of optoelectronics;

**Stronski A.V.** – Doctor of Physical and Mathematical Sciences, Leading Researcher of the Department of Optoelectronics;

**Shportko K.V.** – Doctor of Physical and Mathematical Sciences, Senior Researcher of the Department of Sensory Systems.

- [1] K. Tanaka, *Light-induced anisotropy in amorphous chalcogenide*, Science 277, 1786 (1997); <https://doi.org/10.1126/science.277.5333.1786>.
- [2] A. Stronski, *Production of metallic patterns with the help of high-resolution inorganic resists* In : «Microelectronic Interconnections and Assembly», NATO ASI Series, 3:High Technology, 54, G.Harman@P.Mach, (Eds), Kluwer academic publishers, Netherlands, 263 (1998).
- [3] I.D. Aggarwal, J.S. Sanghera, *Development and applications of chalcogenide glass optical fibers at NRL*, JOAM, 4 (3), 665 (2002); <https://doi.org/10.1080/01468030050058811>.
- [4] A.V. Stronski, M. Vlček, *Photosensitive properties of chalcogenide vitreous semiconductors in diffractive and holographic technologies applications*, JOAM, 4 (3), 699 (2002).
- [5] D. Lezal, *Chalcogenide glasses—survey and progress*, J. Optoelectron. Adv. Mater., 5(1), 23 (2003); [https://doi.org/10.1016/S0022-3093\(03\)00417-4](https://doi.org/10.1016/S0022-3093(03)00417-4).
- [6] S. Kokenyesi, *Amorphous chalcogenide nano-multilayers: research and development*, JOAM, 8(6), 2093 (2006).
- [7] S. Albert, E. Barthelemy, C. Vigreux, A. Pradel, M. Barillot, *Fabrication of far infrared rib waveguides based on Te-Ge-Ga films deposited by co-thermal evaporation*, Advances in Optical Thin Films III, edited by Norbert Kaiser, Michel Lequime, H. Angus Macleod Proc. of SPIE 7101 (7101), 1 (2008); <https://doi.org/10.1117/12.797643>.
- [8] E. Barthélémy, C. Vigreux, G. Parent, M. Barillot, and A. Pradel, *Telluride films and waveguides for IR integrated optics*, Phys. Status Solidi C, 1 (2011); <https://doi.org/10.1002/pssc.201084126>.
- [9] C. Vigreux, E. Barthélémy, L. Bastard, J.-E. Broquin, S. Ménard, M. Barillot, G. Parent, and A. Pradel *Fabrication and testing of all-telluride rib waveguides for nulling interferometry*, Optical Materials Express, 1(3), 357 (2011); <https://doi.org/10.1364/OME.1.000357>.
- [10] Huijuan Xu, Yuju He, Xunsi Wang, Qihua Nie, Peiquan Zhang, Tiefeng Xu, Shixun Dai, Xianghua Zhang, Guangming Tao, *Preparation of Low-loss Ge<sub>15</sub>Ga<sub>10</sub>Te<sub>75</sub> chalcogenide glass for far-IR optics applications*, Inf. Phys. Techn., 65 (4-5), 77 (2014); <https://doi.org/10.1016/j.infrared.2014.03.008>.

- [11] A. Stronski, E. Achimova, O. Paiuk, A. Meshalkin, V. Abashkin, O. Lytvyn, S. Sergeev, A. Prisacar, P. Oleksenko, G. Triduh, *Optical and electron-beam recording of surface relief's using Ge<sub>5</sub>As<sub>3</sub>Te<sub>5</sub>-Se nanomultilayers as registering media*, J. Nano. Res., 39, 96 (2016); <http://dx.doi.org/10.4028/www.scientific.net/JNanoR.39.96>.
- [12] Weike Wang, Liang Li, Zhitao Zhang, Jiyong Yang, Dongsheng Tang, and Tianyou Zhai, *Ultrathin GaGeTe p-type transistors*, Appl. Phys. Lett. 111, 203504 (2017); <https://doi.org/10.1063/1.4998350>.
- [13] A. Stronski, E. Achimova, O. Paiuk, A. Meshalkin, A. Prisacar, G. Triduh, P. Oleksenko, P. Lytvyn, *Direct Magnetic Relief Recording Using As<sub>40</sub>S<sub>60</sub>:Mn–Se Nanocomposite Multilayer Structures*, Nanoscale Research Letters, 12 (1), 286 (2017); <https://doi.org/10.1186/s11671-017-2060-6>.
- [14] A. Stronski, L. Revutska, A. Meshalkin, O. Paiuk, E. Achimova, A. Korchovyi, K. Shportko, O. Gudymenko, A. Prisacar, A. Gubanova, G. Triduh, *Structural properties of Ag–As–S chalcogenide glasses in phase separation region and their application in holographic grating recording*, Optical Materials, 94, 393 (2019); <https://doi.org/10.1016/j.optmat.2019.06.016>.
- [15] M. Bokova, A. Tverjanovich, C. J. Benmore, D. Fontanari, A. Sokolov, M. Khomenko, M. Kassem, I. Ozheredov, and E. Bychkov, *Unraveling the Atomic Structure of Bulk Binary Ga–Te Glasses with Surprising Nanotectonic Features for Phase-Change Memory Applications* ACS, Appl. Mater. Interfaces, 13, 37363 (2021); <https://doi.org/10.1021/acsami.1c09070>.
- [16] M. Wuttig, *Phase change materials: towards a universal memory?* Nat. Mater., 4, 265 (2008).
- [17] K. C. Mandal, R. M. Krishna, T. C. Hayes, P. G. Muzykov, S. Das, T. S. Sudarshan and S. Ma, *Layered GaTe crystals for radiation detectors*, IEEE Trans. Nucl. Sci., 58, 1981 (2011); <https://doi.org/10.1109/TNS.2011.2140330>.
- [18] V.I. Min'ko, I.Z. Indutnyy, P.E. Shepeliavyi, P.M. Litvin, *Application of amorphous chalcogenide films for recording of high-frequency phase-relief diffraction gratings*, Journal of Optoelectronics and Advanced Materials, 7 (3), 1429 (2005).
- [19] A.V. Stronski, M. Vlček, *Imaging properties of As<sub>40</sub>S<sub>40</sub>Se<sub>20</sub> layers*, Opto-Electronics Review, 8(3), 263 (2000).
- [20] Y. Sripathi, G. B. Reddy, L.K. Malhotra, *Structural and optical properties of GaGeTe thin films*, Journal of Materials Science: Materials in Electronics, 2, 109 (1991); <https://doi.org/10.1007/bf00694761>.
- [21] M. Julien-Pouzol, S. Jaulmes, M. Guittard, F. Alapini, *Monotellurure de Gallium, GaTe*. Acta Crystallogr., B, 35, 2848 (1979); <https://doi.org/10.1107/S0567740879010803>.
- [22] T.E. Faber & J. M. Ziman, *A theory of the electrical properties of liquid metals*, Philosophical Magazine, 11(109), 153 (1965); <https://doi.org/10.1080/14786436508211931>.
- [23] N. E. Cusack, & D. L. Stein., *The Physics of Structurally Disordered Matter: An Introduction*, Physics Today, 41(12), 110 (1988), IOP Publishing Ltd., Bristol, England, 1987; <https://doi.org/10.1063/1.2811678>.
- [24] A. Szczygielska, A. Burian, J.C. Dore, V. Honkimki & S. Duber., *Local structure of saccharose- and anthracene-based carbons studied by wide-angle high-energy X-ray scattering*, Journal of Alloys and Compounds, 362(1-2), 307 (2004); [https://doi.org/10.1016/s0925-8388\(03\)00604-2](https://doi.org/10.1016/s0925-8388(03)00604-2).
- [25] T. Proffen, S. J. L. Billinge, T. Egami, and D. Louca, *“Structural analysis of complex materials using the atomic pair distribution function – a practical guide”*, Z. Krist., 218, 132 (2003).
- [26] J.C. Phillips, *Topology of Covalent Non-Crystalline Solids I: Short-Range Order in Chalcogenide Alloys*, J. Non-Cryst. Solids, 34, 153 (1979); <https://doi.org/10.1524/zkri.218.2.132.20664>.
- [27] N. Ramesh Rao, P.S.R. Krishna, S. Basu, B.A. Dasannacharya, K.S. Sangunni, E.S.R. Gopal, *Structural correlations in GexSe1-x glasses - a neutron diffraction study*, Journal of Non-Crystalline Solids, 240, 221 (1998); <https://rad-gtk.software.informer.com/amp/>.
- [28] Y. Maeda and M. Wakagi, *Ge K-edge extended X-ray absorption fine structure study of the local structure of amorphous GeTe and the crystallization*, Japan. J. Appl. Phys. 30 101 (1991); <https://doi.org/10.1143/JJAP.30.101>.
- [29] Li Jingyu, Peng-Fei Liu, Chi Zhang, Xiaobo Sh, Shujuan Jiang, Weizhen Chen, Huabing Yin, Bao-Tian Wang, *Lattice vibrational modes and phonon thermal conductivity of single-layer GaGeTe*, Materials Science Journal of Materiomics, 6 (4), 723 (2020); <https://doi.org/10.1016/j.jmat.2020.04.005>.
- [30] M. Julien-Pouzol, S. Jaulmes, M. Guittard, F. Alapini, *Monotellurure de Gallium, GaTe*. Acta Crystallogr. B, 35, 2848 (1979); <https://doi.org/10.1107/S0567740879010803>.
- [31] Z. Chaker, G. Ori, M. Boero, C. Massobrio, E. Furet, et al., *First-principles study of the atomic structure of glassy Ga<sub>10</sub>Ge<sub>15</sub>Te<sub>75</sub>*, Journal of Non-Crystalline Solids, Elsevier, 498, 338 (2015); <https://doi.org/10.1016/j.jnoncrysol.2018.03.039>.
- [32] Ananth Kumar, Hussein A Mousa, P ChithraLekha, Saleh T Mahmoud and N Qamhieh, *Scrutiny of structural disorder using Raman spectra and Tauc parameter in GeTe<sub>2</sub> thin films*, Journal of Physics: Conf. Series 869, 012018 (2017); <https://doi.org/10.1088/1742-6596/869/1/012018>.
- [33] Chee Ying Khoo, Hai Liu, Wardhana A. Sasangka, Riko I. Made, Nobu Tamura, Martin Kunz, Arief S. Budiman, Chee Lip Gan, Carl V. Thompson, *Impact of deposition conditions on the crystallization kinetics of amorphous GeTe films*, J Mater Sci, 51, 1864 (2016); <https://doi.org/10.1007/s10853-015-9493-z>.
- [34] KS Andrikopoulos, SN Yannopoulos, GA Voyiatzis, AV Kolobov, M Ribes, J Tominaga, *Raman scattering study of the a-GeTe structure and possible mechanism for the amorphous to crystal transition*, J Phys 18 (3), 965 (2006); <https://doi.org/10.1088/0953-8984/18/3/014>.

- [35] KS Andrikopoulos, SN Yannopoulos, AV Kolobov, P Fons, J Tominaga, *Raman scattering study of GeTe and Ge<sub>2</sub>-Sb<sub>2</sub>Te<sub>5</sub> phase-change materials*, J Phys.Chem Solids, 68(5–6), 1074 (2007); <https://doi.org/10.1016/j.jpcs.2007.02.027>.
- [36] R Mazzarello, S Caravati, S Angioletti-Uberti, M Bernasconi, M Parrinello, *Signature of tetrahedral Ge in the Raman spectrum of amorphous phase-change materials*, Phys Rev Lett., 104(8), 085503 (2010); <https://doi.org/10.1103/PhysRevLett.104.085503>.
- [37] C. Vigreux, M.V. Thi, R. Escalier, G. Maulion, R. Kribich, A. Pradel, *Channel waveguides based on thermally co-evaporated Te–Ge–Se films for infrared integrated optics*, J. Non-Cryst. Solids, 377(10), 205 (2013); <https://doi.org/10.1016/j.jnoncrysol.2012.11.037>.
- [38] S.N. Yannopoulos, G.A. Voyiatzis, A.V. Kolobov, M. Ribes, *Raman scattering study of the a-GeTe structure and possible mechanism for the amorphous to crystal transition*, J. Phys.:Condens. Mater., 18(3), 965 (2006); <https://doi.org/10.1088/0953-8984/18/3/014>.
- [39] F. J. Manjón, S. Gallego-Parra, P. Rodríguez-Hernández, A. I. Alfonso Muñoz, C. Drasar, V. Muñoz-Sanjose and O. Oeckler, *Anomalous Raman Modes in Tellurides*, J. Mater. Chem. C, 9, 6277 (2021); <https://doi.org/10.1039/D1TC00980J>.
- [40] B.H.Torrie, *Raman spectrum of tellurium*, Solid State Communications 8, Issue 22, 15 November, 1899 (1970), [https://doi.org/10.1016/0038-1098\(70\)90343-1](https://doi.org/10.1016/0038-1098(70)90343-1).
- [41] Ning Dong, Yimin Chen, Ningning Wei, Guoxiang Wang, Rongping Wang, Xiang Shen, Shixun Dai, Qiuhua Nie, *Optical and structural properties of Ge-Ga-Te amorphous thin films fabricated by magnetron sputtering*, Infrared Physics & Technology, 86, 181 (2017); <https://doi.org/10.1016/j.infrared.2017.09.008>.
- [42] I. Voleská, J. Akola, P. Jóvári, J. Gutwirth, T. Wágner, T. Vasileiadis, S.Yannopoulos, R. Jones, *Structure, electronic, and vibrational properties of glassy Ga<sub>11</sub>Ge<sub>11</sub>Te<sub>78</sub>: experimentally constrained density functional study*, Phys. Rev. B, 86 (9), 094108 (2012).
- [43] S. Sen, E.L. Gjersing, B.G. Aitken, *Physical properties of Ge<sub>x</sub>As<sub>2x</sub>Te<sub>100-3x</sub> glasses and Raman spectroscopic analysis of their short-range structure*, J. Non-Cryst. Solids, 356(41–42), 2083 (2010); <https://doi.org/10.1016/j.jnoncrysol.2010.08.013>.
- [44] P. Neřmec, V. Nazabal, M. Dussauze, H.L. Ma, Y. Bouyrie, X.H. Zhang, *Ga–Ge–Te amorphous thin films fabricated by pulsed laser deposition*, Thin Solid Films, 531(1), 454 (2013); <https://doi.org/10.1016/j.tsf.2013.01.096>.
- [45] J. Sun, Q. Nie, X. Wang, S. Dai, X. Zhang, B. Bureau, C. Boussard, C. Conseil, H.Ma, *Structural investigation of Te-based chalcogenide glasses using Raman spectroscopy*, Inf. Phys. Technol., 55(4), 316 (2012); <https://doi.org/10.1016/j.infrared.2012.03.003>.
- [46] AS Pine, G Dresselhaus, *Raman spectra and lattice dynamics of tellurium*, Phys Rev B, 4(2), 356 (1971); <https://doi.org/10.1103/PhysRevB.4.356>.

М.В.Попович, О.В.Стронський, К.В. Шпортько

## Структурні властивості стекол Ga<sub>11.7</sub>Ge<sub>14.1</sub>Te<sub>74.2</sub>

Інститут фізики напівпровідників ім.В.Є. Лашкарьова НАН України, Київ, Україна, [Niva94@ukr.net](mailto:Niva94@ukr.net)

У цій роботі аморфні сплави Ga<sub>11.7</sub>Ge<sub>14.1</sub>Te<sub>74.2</sub> досліджено методами рентгенівської дифракції та рамановської спектроскопії. Експериментальні рентгенівські дифрактограми були використані для розрахунків функцій радіального розподілу, які вказують положення довжин зв'язку найближчого сусіда r<sub>1</sub>=2,67 Å і довжини зв'язку другого сусіда r<sub>2</sub> = 4,27 Å. Подібні значення r<sub>1</sub> спостерігалися для стекол Ga-Ge-Te інших складів. Смуги, які спостерігаються в спектрах комбінаційного розсіювання зразків Ga<sub>11.7</sub>Ge<sub>14.1</sub>Te<sub>74.2</sub> показують, що це скло містить різні нанофази, що можна пояснити за допомогою режимів коливань, властивих склам Ga-Te і Ge-Te, а також півкам. Дослідження композиційних залежностей характерних складових інтенсивностей раманівських смуг, які змінюються зі зміною складу, слід вивчати для отримання кращого розподілу раманівських смуг.

**Ключові слова:** халькогенідні стекла; рентгеноструктурний аналіз; функція радіального розподілу; Раманівська спектроскопія; нанофази.